Field-based Single Plant Phenotyping for Plant Breeding

Jared Crain[1*], Xu Wang[1,2], Byron Evers[1], Jesse Poland[1,3,*]

[1] Dep. Plant Pathology, Kansas State University, 4024 Throckmorton Plant Sciences Center, 1712 Clafin Road, Manhattan KS, USA 66506;

[2] Current address Department of Agricultural and Biological Engineering, University of Florida, IFAS Gulf Coast Research and Education Center, Wimauma, Florida, 33598

[3] Center for Desert Agriculture, King Abdullah University of Science and Technology, Thuwal Saudi Arabia. Received _____.

[*]Corresponding author:jcrain@ksu.edu; jpoland@ksu.edu, jesse.poland@kaust.edu.sa

Author ORCID:

Jared Crain (0000-0001-9484-8325)

Xu Wang (0000-0002-7144-6865)

Byron Evers (0000-0003-1840-5842)

Jesse Poland (0000-0002-7856-1399)

Single Plant Analysis for Breeding

Core ideas: (3-5 impact statements, 95 char max for each)

- Development of a high-throughput single plant field-based phenotyping pipeline and analysis
- Single plant and full plot traits had common loci identified by GWAS
- Variable correlations were found between single plants and full plots across traits and years
- Challenges of genotype-by-environment interaction to accurately identify superior plants
- Potential for using high-throughput data for early generation plant breeding

Abbreviations: AM, association mapping; BLUE, best linear unbiased estimator; GBS, genotyping-by-sequencing; GS, genomic selection; GWAS, genome-wide association analysis; GxE, genotype by environment; HTP, high-throughput phenotyping; NGS, next generation sequencing; NDVI, normalized difference vegetation index; NIR, near infrared; SNP, single nucleotide polymorphism; SPAM, single plant association mapping; UAV, unmanned aerial vehicle

Abstract

High-throughput phenotyping (HTP) has the potential to revolutionize plant breeding by providing scientists with exponentially more data than was available through traditional observations. Even though data collection is rapidly increasing, the optimum use of this data and implementation in the breeding program has not been thoroughly explored. In an effort to apply HTP to the earliest stages of a plant breeding program, we extended field-based HTP pipelines to evaluate and extract data from spaced single plants. Using a panel of 340 winter wheat lines planted in full plots and grid-spaced single plants for two growing seasons, we evaluated relationships between single plants and full plot yields. Normalized difference vegetation index (NDVI) was collected multiple times through the growing season using an unmanned aerial vehicle. NDVI measurements during grain filling stage from both single plants and full plots were typically positively associated with their respective grain yield with correlation ranging from -0.22 to 0.74. The relationship between single plant NDVI and full plot yield, however, was variable between seasons ranging from -0.40 to 0.06. A genome wide association analysis (GWAS) identified the same significant markers for traits measured in both full plots and single plots, but also displayed variability between growing seasons. Strong genotype by environment interactions could impede selection on quantitative traits, yet these methods could provide an effective tool for plant breeding programs to quickly screen early-generation germplasm especially for qualitative traits. Effective use of early-generation, affordable HTP data could improve overall genetic gain in plant breeding.

1 Introduction

In the twentieth century, the Green Revolution led to more than doubling production of many cereal grains (Pingali, 2012) while preventing large swaths of land from being degraded by agriculture (Stevenson et al., 2013). Today, agriculture faces a myriad of challenges including feeding an increasing population, more demand for agriculture products due to changing consumptions patterns, climate change, and limited resources to increase agriculture productivity (The Royal Society, 2009). Meeting these needs requires an increased agriculture productivity of which plant breeding can play an integral role. Modern plant improvement is focused to improve agronomic performance of plants for food, fiber, feed, and fuel.

While the premise of plant breeding to improve populations has not changed, the tools of plant breeders has rapidly expanded in the 21st century. Meuwissen et al. (2001) proposed whole genome prediction (genomic selection, GS) using dense genetic markers. This method functions by ensuring dense molecular markers are linked to quantitative trait loci and utilizing a training population that has been genotyped and phenotyped. Using the training population, a model can be developed that can predict individuals that have only been genotyped, potentially eliminating the need for large scale, costly field trials and phenotyping (Heffner et al., 2010; Poland, 2015). With the advent of next-generation sequencing (NGS) and the rapid decline in marker cost, GS has become a tractable

plant breeding method for many staple crops including wheat (Poland et al., 2012b; Rutkoski et al., 2014; Belamkar et al., 2018), maize (Zhang et al., 2017), sorghum (Muleta et al., 2019), potato (Enciso-Rodriguez et al., 2018) as well as forage and tree species (Lin et al., 2014). Genomic selection has been used to increase yield (Crain et al., 2021a), improve disease resistance (Rutkoski et al., 2012; Enciso-Rodriguez et al., 2018), and to speed the domestication of new crops (Crain et al., 2020). In many breeding applications, GS reduces the breeding cycle timeline improving genetic gains per unit time (Heffner et al., 2009).

A key component of GS is having an adequate training population that has been both genotyped and phenotyped. With the potential to use NGS for applications of marker and gene discovery for both model and non-model plants (Bräutigam and Gowik, 2010), phenotyping quickly became a limiting factor for genetic studies and plant breeding (White et al., 2012; Cobb et al., 2013; Poland, 2015). GS has led to a paradigm shift from phenotyping for plant evaluation and selection to phenotyping for GS model development with a greater emphasis on precision of measurement as well as phenotyping different sets of lines (Heffner et al., 2009; Cobb et al., 2013). For successful implementation of advanced breeding methodologies including GS, phenotyping has emerged as the critical bottleneck.

Realization of the phenomic bottleneck has led to the relatively new discipline of phenomics (Furbank and Tester, 2011). Over the past decade a variety of tools have been developed to aid in high-throughput phenotyping (HTP) of plants. Phenomics now offers an array of tools from aerial platoforms (Liebisch et al., 2015; Haghighattalab et al., 2016; Singh et al., 2019) to ground-based vehicles (Deery et al., 2014; Andrade-Sanchez et al., 2014; Barker et al., 2016) and even pushcarts (White and Conley, 2013; Crain et al., 2016). These phenotyping platforms can collect a variety of data from the electromagnetic spectrum including visible imagery, hyperspectral data, and canopy temperature (reviwed in Fahlgren et al., 2015), which can be assigned to plots or plants providing data to evaluate genotypes (Haghighattalab et al., 2016; Wang et al., 2016).

The advances in HTP platforms have provided massive data sets that can be used to dissect plant growth and architecture (Busemeyer et al., 2013; Crain et al., 2017), identify quantitative trait loci (Tanger et al., 2017), and be used for GS and breeding decision making (Rutkoski et al., 2016; Crain et al., 2018). In addition to complementing genomic data, phenomics data is also being considered for directly making prediction and selection decisions in breeding. For example, Rincent, *et al.* (2018) provided proof of concept of phenomic selection using near infrared spectroscopy to generate predictions as accurate as predictions using molecular markers (GS) in both wheat and poplar (*Populus nigra* L.). Work by Krause *et al.* (2019) also found that phenomic data could provide equivalent accuracy as molecular data for predictions in wheat. Phenomic predictions have also been used successfully in soybean (Parmley et al., 2019) with prediction accuracy equivalent to GS (Zhu et al., 2021). Regardless of

whether phenotypic data is used in conjunction with molecular markers or independently, these methods are providing novel methods for plant breeders to increase genetic gains.

Even though systems now exist to collect dense phenotypic and genotypic data, less work has been performed on how to best integrate these methods into a breeding program. While both Rutkoski *et al.* (2016) and Crain *et al.* (2018) concluded that adding phenotypic data could increase breeding efficiency in elite wheat breeding germplasm, both studies used material from the advance yield trials at the International Maize and Wheat Improvement Center. While representative of a typical breeding program, these trials were advanced lines that had already progressed through multiple stages of selection and were near the end of the breeding cycle. This material would have been inbred to at least the F_5 generation and there would have been additional time spent on seed increases through preliminary yield trials (Rajaram et al., 2002). In an effort to introduce phenotyping earlier into the breeding cycle Krause *et al.* (2020) phenotyped breeding lines in unreplicated small plots, which represents the first field plot evaluation as inbred lines derived from single plants. While this enabled high-throughput phenotyping earlier in the plant breeding cycle, multiple rounds of inbreeding and visual selection had already occurred, representing significant time and resource inputs, while potentially decreasing the impact of advanced tools for selection in the breeding pipeline.

As any new technology can shift breeding activities throughout the cycle, maximum genetic gain will be achieved by optimally allocating resources within the plant breeding program given the balance of selection accuracy, selection intensity and cost of evaluation. Resource allocation is a challenging problem that encompasses all stages of the breeding program and fluctuates as key selection targets such as grain yield and disease resistance vary throughout the stages of the breeding cycle (Heslot et al., 2015). For example, thousands of lines are often evaluated during the inbreeding stage of the cycle, yet only tens or hundreds may be evaluated in full, replicated plots later in the breeding cycle where the evaluations are more accurate yet more costly per line. The emergence of molecular tools (GS), HTP, and environmental data has brought new focus on how plant breeding programs can successfully implement and exploit these advances (Crossa et al., 2021).

A critical stage in the breeding pipeline is early generation testing of single plants, which could be a powerful entry point of improved selection methodologies within breeding programs. To date, early generation selection on single plants in wheat is typically visual and has not routinely included advanced tools (Rajaram et al., 2002). Thus, the potential of increasing selection gains in this stage of the breeding program has created strong research interest. Fischer and Rebetzke (2018) reviewed literature of early generation phenotyping in cereal grains and identified areas where selection would be possible in early stages of the breeding cycle. Many traits are indirectly related to grain yield, including some traits that may scale to the size of breeding programs including plant

height, harvest index, kernel weight, and leaf angle (Quail et al., 1989). Additionally, other traits such as carbon isotope discrimination (Rebetzke et al., 2002) and stomatal aperture traits (Condon et al., 2008) were correlated with yield; however, there is no current viable methods to scale these to the level of commercial breeding programs. Efficient and precise measurement of these traits could be used to enhance genetic gains at later stages of the breeding cycle.

High-throughput phenotyping methods could provide an opportunity to quantitatively evaluate early generation breeding material, where insufficient seed is available for large plots. With the right approach, such HTP screening could scale to the level of breeding programs to evaluate and select in populations of thousands to millions of individual plants (Deery and Jones, 2021). In addition, HTP measurements could provide a level of precision that is not available through visual or qualitative assessments (Tanger et al., 2017; Duddu et al., 2019). This could be useful for programs working with inbreeding as well as outcrossing species. Our objectives were to (a) adopt the methods of field-based HTP from plot level to single plant level, (b) evaluate the relationship between HTP measurements in single plants and full yield plots of the same genotype, and (c) provide proof of concept of early generation HTP within breeding programs.

2 Materials and Methods

2.1 Plant Material

We used 340 unique lines of which 274 have been used in the hard winter wheat association mapping panels described by Guttieri *et al.* (2015) and Grogan *et al.* (2016). These lines are representative of pedigrees and germplasm grown in the Great Plains regions and include lines developed in Colorado, Kansas, Montana, North Dakota, Nebraska, Oklahoma, South Dakota, and Texas from both public and private breeding programs. The majority of the lines are from release in the years of 1960-2010, with several historic lines (Bison, Cheyenne, Comanche, Kharkof, Kiowa, Tascosa, and Wichita). The remaining 66 lines represented newer material and were additional advanced lines and cultivars from the region.

2.2 Experimental Design

Field trials were conducted using all lines for two growing years in Kansas. The 2019-2020 season was at the Rocky Ford Experiment station (39 ° 13'48.82" N, 96 ° 34'41.87" W), while the 2019-2020 season was grown at the Ashland Bottoms Experiment Station (39 ° 08'19.07" N, 96 ° 38'21.00" W). To allow single plant comparisons to full yield plots, all entries were planted in two separate trials.

2.2.1 Association Mapping Panel

The association mapping (AM) panel was planted as a two replicate, complete block design where experimental plots were 2.4 m x 1.4 m (3.36 m^2). Each

plot consisted of six rows on 20 cm spacing and was seeded at a rate of 1.25 g m^{-2}. Plots were sown within the normal planting time for winter wheat in KS (24 October 2018, and 17 October 2019), and management practices for optimal yield were maintained. Herbicide (Finesse®, 0.03 kg ha^{-1} chlorsulfuron + metsulfuron-methyl, and MCPA 0.84 kg ha^{-1} 4-chloro-2-methylphenoxy) was applied on April 9, 2019. Grain yield was harvested using a Kincaid 8XP plot combine (Kincaid Manufacturing., Haven, KS, USA). Grain weight was moisture corrected to 12% and recorded for each plot using a Harvest Master Classic GrainGage and Mirus harvest software (Juniper Systems, Logan, UT, USA).

2.2.2 Single Plant Association Mapping Panel

To replicate the situation of genetically distinct single plants during early stages of a breeding program, all AM entries were also planted in the single plant association mapping (SPAM) trials. The SPAM trial consisted of a four replicate complete block design, where single plants were grid spaced with 50 cm in 2018-2019. To provide better separation of individual plants, 2019-2020 trials were spaced on a 70 cm grid. Single seeds were started in greenhouse plugs on October 12, 2018 and October 8, 2019 respectively. Plants were allowed to grow to the two-leaf stage before being field transplanted on November 5, 2018 and October 25, 2019. Starting plants in plugs insured that only one seed per entry was grown, after plants were transplanted to the field, management was the same for both AM and SPAM trials. At maturity, single plants were hand-harvested and threshed individually to obtain final plant grain weight.

2.3 Phenotypic Data Collection

Several hand-measured phenotypic parameters were collected in both the AM and SPAM panels. Heading date (growth stage 55, Zadoks et al., 1974) was recorded as the days after January 1 for each respective growing year. Spikelets per spike and spike length, excluding the awns, were measured on three (sub-samples) random spikes from the same plant in the SPAM panel and different plants in the AM panel. Number of fertile tillers, excluding any secondary or non-fertile tillers when the primary tillers reached physiological maturity, were counted for each plant in SPAM. In the AM panel tillers m^{-2} was determined by counting the number of tillers in a 50 cm length for the middle two rows of the AM plots. Tiller count was then transformed to spikes m^{-2} using the following formula:

$$\text{spikes } m^{-2} = \frac{\text{tiller count}}{2{*}0.5\ m{*}0.20\ m} \quad \text{Equation 1}$$

where 2 rows of 0.5m length were counted with a 0.20m row spacing. In 2019, two separate tiller counts were completed per plot, but due to labor constraints in 2020 only one representative count of tillers were performed per plot. All field phenotypic data was digitally recorded in Field Book app (Rife and Poland, 2014). After harvest, thousand kernel weight was measured for all SPAM and AM plots.

2.4 High-Throughput Phenotyping Data

High-throughput phenotyping data was collected during the spring growing season from AM and SPAM experiments each year using DJI Matrice 100 (DJI, Shenzhen, China) unmanned aerial vehicles (UAV) (quadcopter). The UAV was equipped with MicaSense RedEdge-M multispectral camera (MicaSense Inc. United States) that captured blue, red, green, near infrared (NIR), and red edge wavelengths allowing the calculation of vegetation indices including normalized difference vegetation index (NDVI) (Rouse et al., 1974):

$NDVI = \frac{NIR - Red}{NIR+Red}$ Equation 2

Following the methods of Haghigattalab *et al.* (2016) and Wang *et al.* (2020), white square tiles (30 cm x 30 cm) ground control points were distributed in the trials to improve geospatial accuracy and surveyed with an Emlid Reach RS (Emlid Ltd. Hong Kong), Real-Time Kinematic (RTK) Global Navigation Satellite System (GNSS). Similar to Wang *et al.* (2020) flight speed and elevation were chosen to maintain a desired 80% overlap between parallel flight paths for orthomosaic image stitching. Flight missions were created using the CSIRO mission planner application (https://uavmissionplanner.netlify.app/) and executed using the Litchi Mobile App (https://flylitchi.com/). The AM panel was flown at a height of 20 m above ground, while the SPAM panel was flown at a lower 10 m above ground corresponding to a ground resolution of approximately 6 mm pixel^{-1}. Flight speed for all AM trials was 2.0 m s^{-1} and SPAM trials were flown at 1.3 m s^{-1} with all flights occurring within 1.5 hours of solar noon (typically between 12:00 pm and 3:00 pm). A semi-automated image processing pipeline developed by Wang et al. (2020) was used to ortohomosaic all images and extract plot level data (NDVI). The processing pipeline used Agisoft PtotoScan Python API (Version 1.4.0, Agisoft LLC, Russia) to create the orthomosaiced images, followed by trait extraction using Python scripts.

2.5 Statistical Analysis

All statistical analysis were conducted in R version 4 (R Core Team, 2020). All subsample data, multiple measurements of spikelets spike^{-1}, spike length, and spike number on each plot, were averaged into a single phenotype before analysis. Models were fit separately for the AM and SPAM trials using a linear mixed model in the *lme4* (Bates et al., 2015) R package. Best linear unbiased estimators (BLUEs) for each line were obtained from the *emmeans* (Lenth, 2020) R package with data combined across years using Equation 3:

$y_{\text{ijk}} = \mu + g_i + t_j + r_{k(j)} + \beta_{l_{\text{ijk}}} + \varepsilon_{\text{ijk}}$ Equation 3

where y_{ijk} is the phenotype, μ is the overall mean for the trait of interest, g_i is the fixed effect for genotype *i*, t_j is a random effect for year (2018-19 or 2019-20), independently and identically distributed $t_j \sim \text{N}(0, \sigma_j^2)$, $r_{k(j)}$ is the random effect for the k^{th} replicate (AM k = 1-2, SPAM k = 1-4) nested within the j^{th} growing season distributed as $r_k \sim \text{N}(0, \sigma_l^2)$, $\beta_{l_{\text{ijk}}}$ is a fixed covariate for heading date for each genotype, year, replicate combination, and ε_{ijk} is the residual effect for the i^{th} genotype, j^{th} year, and k^{th} replicate distributed as $\varepsilon_{\text{ijk}} \sim \text{N}(0,$

σ^2_ε). To calculate heritability for traits across the two growing years, the fixed genotype effect was changed to a random effect. Broad sense heritability (H^2) or repeatability (Piepho and Möhring, 2007) was then calculated according to Holland et al. (2010) as:

$$H^2 = \frac{\sigma^2_g}{\sigma^2_g + \frac{\sigma^2_{\text{gy}}}{y} + \frac{\sigma^2_\varepsilon}{\text{yr}}} \text{ Equation 4}$$

where σ^2_g is the genotypic variance, σ^2_{gy} is the variance attributed to genotype by year (genotype by environment [GxE]) variance, and σ^2_ε is the residual error variance from Eqn. 3, y is the number of years (2), and r is the number of replicates (AM = 2, SPAM = 4). Data was also analyzed within each year by dropping the year term from Eq. 3 resulting in Eq. 5

$$y_{\text{ik}} = \mu + g_i + r_k + \beta_{l_{\text{ik}}} + \varepsilon_{\text{ik}} \text{ Equation 5}$$

where all terms are equivalent to Eq. 3. Broad sense heritability was calculated similarly by dropping the genotype by year term as Eq. 6:

$$H^2 = \frac{\sigma^2_g}{\sigma^2_g + \frac{\sigma^2_\varepsilon}{r}} \text{ Equation 6}$$

with all terms being defined as Eq. 4.

2.6 Genotypic Data

A total of 321 unique lines from the AM panel detailed by Guttieri *et al.* (2015) and Grogan *et al.* (2016) were genotyped using genotyping-by-sequencing (GBS). Single nucleotide polymorphic (SNP) markers were discovered with GBS following the protocols of Poland *et al.* (2012a) using the TASSELv2 pipeline (Glaubitz et al., 2014) and the Chinese Spring reference genome (International Wheat Genome Sequencing Consortium, 2014). Samples were sequenced on multiple lanes of Illumina Hi Seq to increase sample coverage, with three million average good-barcoded reads per sample (range 876286 – 12001293). A total of 112,248 unique SNPs were identified across all samples. Data filtering consisted of removing individual markers with: (a) a minor allele frequency $<$ 0.05; (b) percent heterozygous $>$ 0.05; (c) percent missing $<$ 0.5. Beagle version 4.1 was used to impute missing markers with default setting (Browning and Browning, 2016). The final genotypic data set for evaluating population structure and genome-wide association analysis (GWAS) consisted of 321 lines and 11,452 SNPs.

2.7 Genomic Analysis

Using the SNP markers and phenotypic data, a GWAS was performed for both the AM and SPAM panels for each growing season. A mixed model following Yu *et al.* (2006) that can account for both population structure and kinship was implemented in the *rrBLUP* (Endelman, 2011) R package as:

$$y = \mathbf{X}\beta + \mathbf{Z}g + \text{S} + e \text{ Equation 7}$$

where y is an n x 1 vector of phenotypes (BLUEs from Eq. 5), β is a p x 1 vector of fixed effects and p is the number of effects for population structure, $\mathbf{X}$ is an n x p design matrix for population structure, g is an n x 1 vector of random genetic effects representing kinship, $\boldsymbol{Z}$ is an n x n genomic relationship matrix, τ is the fixed marker effect for each marker tested individually and S is an n x 1 vector of genotypes for the marker being tested, and e is an n x 1 vector of residuals. The genomic relationship matrix was calculated with the *A.mat* function in *rrBLUP* package (Endelman, 2011) and according to methods of Endelman and Jannink (2012). The first six principal components ($p = 6$) where each component explained more than 2% of the variation, were used to account for population structure. The P3D 'population parameters previously determined' option was used (Zhang et al., 2010). A false discovery rate of 0.1 was used to identify significant markers within the GWAS (Storey and Tibshirani, 2003) and the *qqman* (Turner, 2017) R package was used for data visualization.

2.8 Data Availability

Phenotypic data, including raw images and analysis scripts are available in the Dryad Digital Repository: doi:10.5061/dryad.w0vt4b8s4

temporary link for peer review: https://datadryad.org/stash/share/SGRdMlrASBRSzIHocMhGdz9fONynvLUN7m8y8LTDbjU

DNA sequence data from genotypes used in this study is available in NCBI Sequence Read Archive (SRA) (https://www.ncbi.nlm.nih.gov/bioproject/) as BioProject accession number PRJNA764168.

3 Results

In order to translate field-based HTP methodology to single plants as well as evaluate the potential for HTP based selection early within the breeding program, we evaluated two growing years of full plot association mapping (AM) and single plant association mapping (SPAM) panels under the same field conditions. Using fixed lines in the SPAM trials enabled us to create an artificial segregating population similar to individual F_2s that could be replicated from year to year. Additionally, having the full AM plots allowed a comparison between data measured on single plants and full plots. Data were collected from the AM and SPAM trials throughout the growing season with HTP data acquisition respectively spanning the growing season from stem elongation to ripening. Using UAVs equipped with sensors, there were 14 dates of data collection in AM and six in the SPAM trial in the 2018-19 season of which five occurred on the same day for both trials. In 2019-20 there were seven overlapping days of for both AM and SPAM data collection and a total of 11 AM and nine SPAM data sets. The majority of the measurements occurred between mid-April to mid-June each year with approximately 5-10 days between measurement. Each data collection resulted in approximately 700 and 500 images for AM and SPAM that were processed (Figure 1) using a semi-automated pipeline to construct orthomosaic image and extract phenotypic traits. Broad-sense heritability, or repeatability,

for the HTP data was higher for the AM plots than SPAM each season. In addition, H^2 was higher in the 2018-19 season than in 2019-20 with this trend observed for both AM and SPAM experiments (Figure 2, Supplementary Table 1).

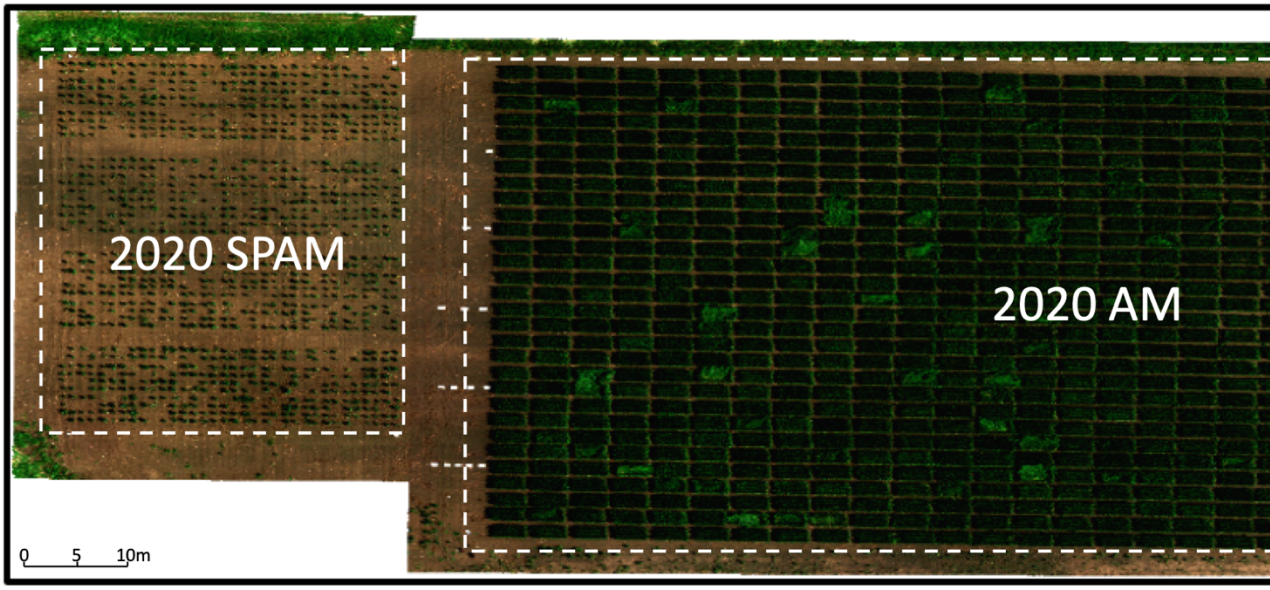

Figure 1. Orthomosaic image of single-spaced planted association mapping (SPAM) and full association mapping (AM) field trials, Manhattan, KS, 2020.

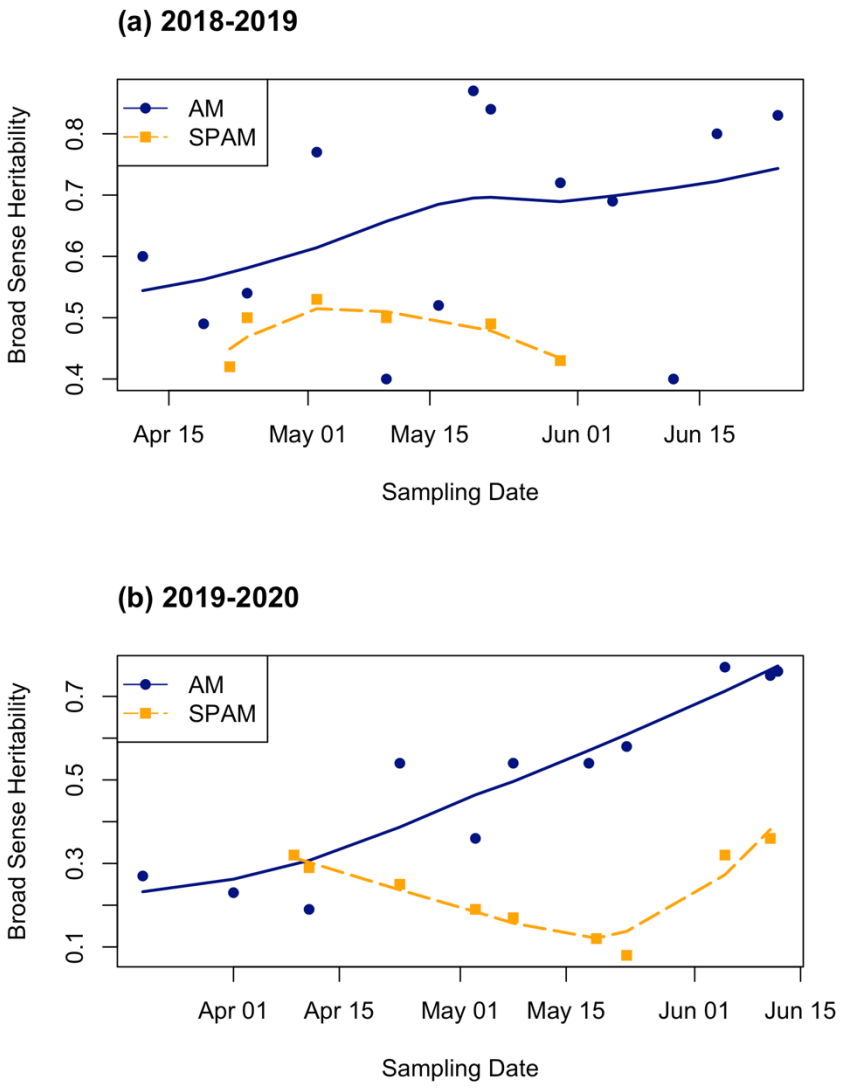

Figure 2. Broad-sense heritability of high-throughput normalized difference vegetation index data collected throughout the 2018-2019 year (a) and 2019-2020 year (b) with an unmanned aerial vehicle in association mapping (AM) and single plant (SPAM) panels, Manhattan, KS. Days of observations are represented by points with smoothed trend lines for multiple days of data collection.

3.1 Association Mapping Panel

Within the AM trials, several hand-measured phenotypes were evaluated to determine their relationship to grain yield. Across both growing years, plant height

was the only trait that had a strong, consistent, negative correlation to grain yield (Figure 3). In the 2020 growing season, yield component traits of spikes m^{-2}, spikelets $spike^{-1}$, and thousand kernel weight were strongly associated with yield; however, in the 2019 season these traits were not significantly correlated to yield (Figure 3). Broad sense heritability for all traits was high at H^2=0.45 or greater, with the exception of spikes m^{-2} having low heritability (Figure 3). Complementing the hand-measurements were the HTP data that was tested for correlation to full plot grain yield. Across both years after mid-April, correlations tended to be positive and significantly associated with grain yield with the strongest correlations occurring after heading (Figure 4, Supplementary Table 2).

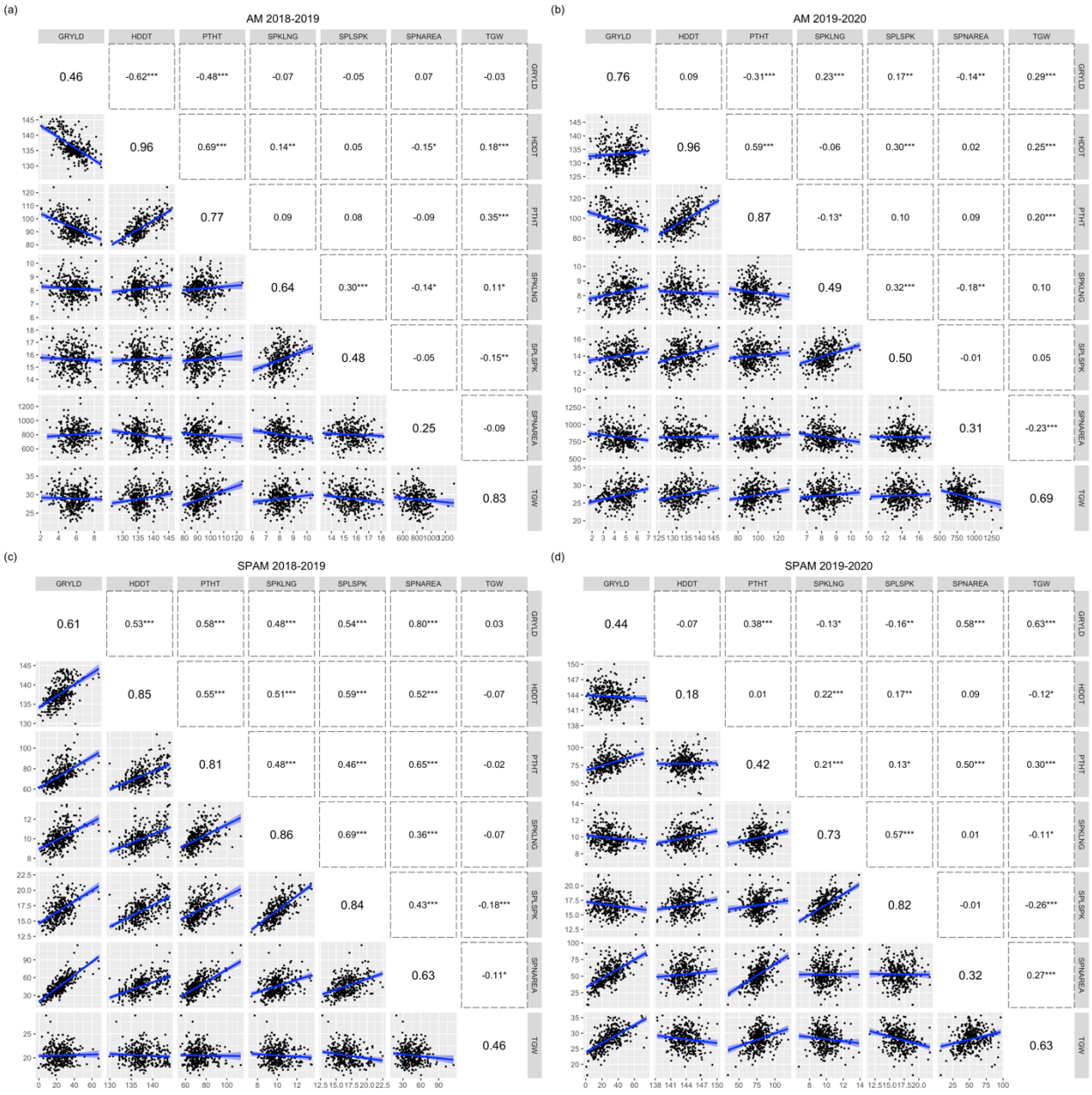

Figure 3. Correlation between grain yield (GRYLD), heading date (HDDT), plant height (PTHT), spike length (SPKLNG), spikelets spike^{-1} (SPLSPK), spikes m^{-2} (SPNAREA), and thousand grain weight (TKW) for full plots (AM, panels a and b) and single plants (SPAM, panels c and d) grown for two growing seasons in Manhattan, KS. The lower triangle in each panel has a scatter plot and line of best fit, the upper panel is the correlation between variable, and the

diagonal is the broad-sense heritability of each trait.

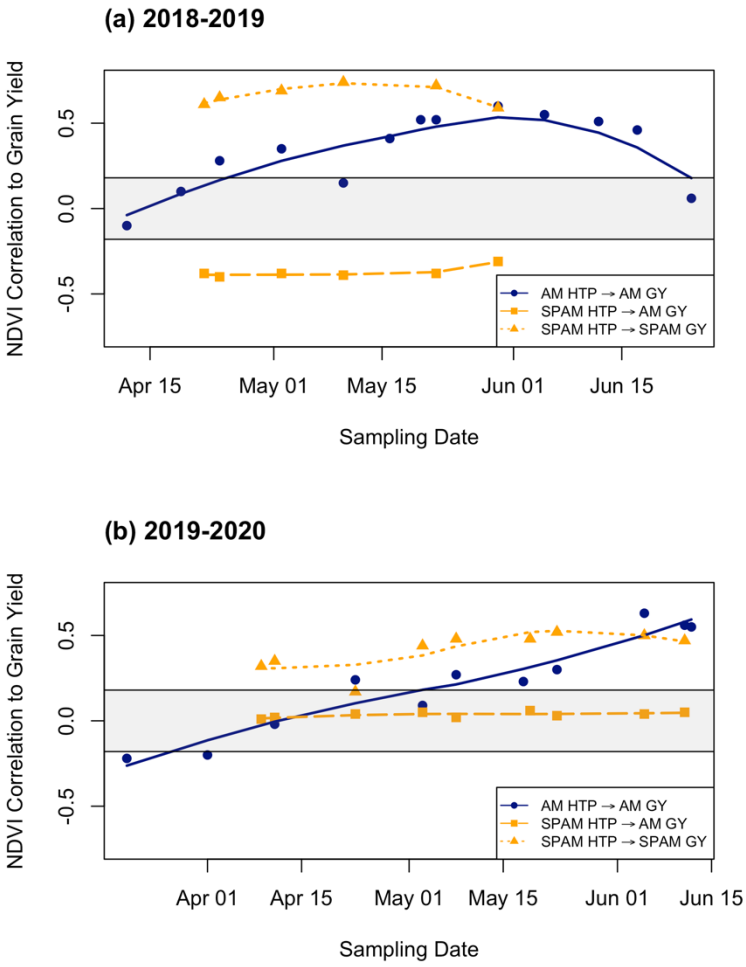

Figure 4. Correlation between normalized difference vegetation index collected with high throughput phenotyping (HTP) and wheat grain yield (GY) for full plots (AM) and single plants (SPAM) for growing years (2018-2019, 2019-2020, panels a and b). The SPAM trial includes both correlation to single plants and the correlation to full plot yields. The area above or below the shaded region represents significant correlation values ($p\text{-}value < 0.001$, n = 330).

3.2 Single Plant Association Mapping Panel

To evaluate the potential of phenotyping and selecting single plants, we collected both hand-measured traits and HTP data in the SPAM trial. In comparison to the full AM plots, plant height was positively associated with yield both

seasons as was the number of spike plant^{-1} (Figure 3). Spikelets spike^{-1} had significant but opposing correlations between the two seasons, and thousand kernel weight was significant in 2020, yet not strongly associated with yield in 2019 (Figure 3). Broad-sense heritability was more variable between years compared to heritability observed in the full plots, yet most traits had $H^2 > 0.4$ (Figure 3). Single plant NDVI was always positively associated with grain yield of the single plants and the correlations were of similar magnitude of correlations observed between full plot grain yield and NDVI (Figure 4).

3.3 Relationship Between Single Plants and Full Plots

Leveraging the fixed lines grown both in the AM and SPAM panels, allowed a comparison of how single plant could be used to predict full plot agronomic characteristics including grain yield. In the 2018-19 season, we found that HTP data collected in the SPAM trials showed a strong and consistently negative correlation (r = -0.40 — -0.31) to full plot grain yield even though there was a positive correlation between single plant grain yield and NDVI (Figure 4). However, in the 2019-20 season, even though single plant yield and NDVI were related, there was no relationship (r = 0.01— 0.05) between single plants and full plot yields (Figure 4).

3.4 Genome-wide Association Analysis

A genome-wide association analysis was used to evaluate genetic architecture of trait expression in both the full plots and single plants. As the lines in each panel were fixed, this allowed us to test if trait expression was controlled under both growing conditions similarly and potentially allow selection on single plants for full plot characteristics. In the 2018-19 growing season spikelets spike^{-1} showed a GWAS peak on chromosome 7A and spike length had high scoring markers on chromosome 2B for both AM and SPAM panels (Figure 5, Supplementary Figure 1). For these same traits, there were no associations found for either panel in 2019-20 season. No significant associations were found for grain yield, thousand kernel weight, or spikes m^{-2} for either season of evaluation. Within the full plot AM panel, an association was found for plant height on chromosome 4B for both growing seasons. While no significant markers were identified within the SPAM panel, the same marker that was identified in the AM panel had one of the highest values each year (Supplementary Figure 2).

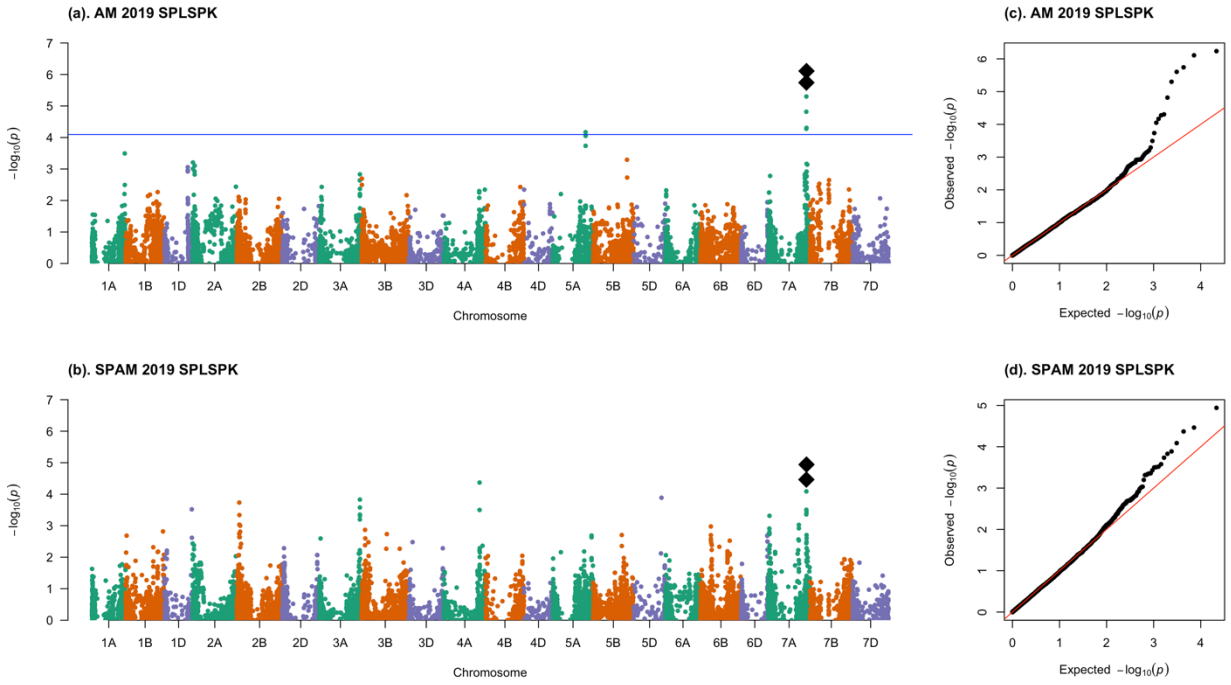

Figure 5. Manhattan plots of spikelets spike^{-1} with phenotypic data taken from full plots (a) and single plots (b). Horizontal blue line is the false discovery rage (FDR = 0.1). The same highest scoring markers in both single plants and full plots have been denoted with black diamonds. Quantile-quantile plots showing the expected and observed residual distribution for each genome-wide association analysis (c and d).

3.5 Genotype by Environment Interaction

Based on our contrasting findings of strong associations between traits in one season and then no association in another season, we evaluated data across years. This allowed us to partition variance components, including GxE, to determine the proportion of genetic and non-genetic effects. Across both years for the AM and SPAM panel, the heritability for grain yield was lower than for individual single seasons suggesting GxE interactions, and this trend carried through to several traits including thousand kernel weight. Across all traits, the proportion of genetic variance was less than 50% of total variation indicating strong environment and year effects complicating potential selection strategies (Figure 6).

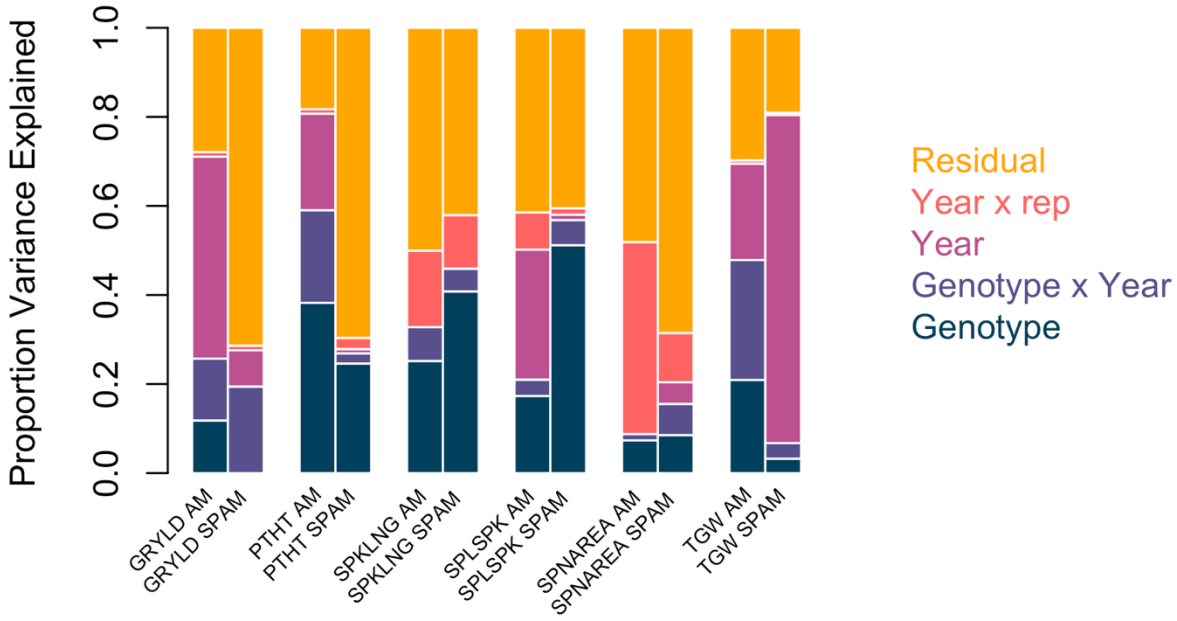

Figure 6. Proportion of variance explained for each type of effect for phenotypic traits collected in full plot (AM) and single plant (SPAM) wheat panels. GRYLD, grain yield; PTHT, plant height; SPKLNG, spike length; SPLSPK, spikelets spike^{-1}, SPNAREA, spike m^{-2}; TGW, thousand kernel weight.

4 Discussion

4.1 Single Plant HTP Analysis

In an effort to extend HTP methodology to the earliest time points in the breeding program, we adapted existing processing and analysis pipelines to extract data from single plants. Our choice of experimental population grown both as single plants and full plots, enabled us to evaluate an artificially created segregating population similar to single F_2 plants that could provide an idea of the plasticity that could be observed in single plants for HTP and how that would compare to full plots. The positive correlations between NDVI and grain yield is similar to other research finding where NDVI has been suggested as a selection tool in plant breeding (Babar et al., 2006; Prasad et al., 2007; Crain et al., 2017). While we only assessed NDVI, these methods should be practical for a broad range of phenotypic measurements. For example, UAVs have been used

to quantify plant height (Singh et al., 2019; Volpato et al., 2021), plant diseases (Wu et al., 2019), morphological and physiological traits such as heading date and presence of awns (Wang et al., 2019), and canopy temperature (Tattaris et al., 2016). Although previous research in early-generation plant phenotyping has been promising but limited by volume of phenotyping throughput (reviewed extensively by Fischer and Rebetzke, 2018), the advent of HTP methodology has opened the possibilities for expanded observation and selection in early generations. Even though our methods were applied to space planted individuals, we expect that continued refinement in algorithms and methodology will allow for evaluation of single plants that are more densely planted and not completely separated.

4.2 Application to Breeding Programs

Many wheat breeding programs have minimal observations of early-generation material such that HTP could provide affordable and accessible data that can help enhance selection decisions. Using pipelined analysis, we envision that breeding programs could collect data on all generations of data while simultaneously making selection decisions. Instead of breeding lines being promoted to yield trials in advanced generations (F_5 or later) with only breeder visual selection during each generation, lines could have multiple cycles of selection through impartial computational methods. As methods are refined, breeders could choose phenotypes that are expressed in single plants and maintained in full plots or optimal HTP phenotypes that are well correlated to full plot yield, even if the trait *per se* is not correlated or important for yield in full plots.

While we observed variable results between single plot yield and full plot yield for correlation of HTP data and grain yield, we did observe several GWAS hits that were similar between the two panels. For example, in 2018-19 season spikelets spike^{-1} both had the same significant markers. In addition, a significant marker for plant height was the same for both growing seasons and panels. This marker on chromosome 4B corresponds to the *reduced height* (*Rht-B1*) locus (Jobson et al., 2019; Chai et al., 2021). These results suggest that selection methods can be developed to identify desired characteristics even in segregating populations. As HTP advances, the opportunity to link desired ideotypes (Donald, 1968) expression to single and full plots will allow breeders to implement enhanced selection on all breeding germplasm.

Based on the changing results between the two growing seasons, we examined the effect of GxE within the growing panels. Decomposition of variance revealed that there were large environmental and GxE effects which could explain the difference observed between years and impede efficient selection decisions. Unfortunately, GxE is a well-known and documented challenge (e.g. De Leon et al., 2016; Elias et al., 2016; Van Eeuwijk et al., 2016) facing plant breeding and effects all stages of plant breeding (Kang, 1997) and evaluation of breeding lines in replicated full plots does not escape the confounding effects of GxE on selection. Even though in our analysis the selection potential has been constrained by GxE, the methods developed may allow for better dissection of GxE results.

In addition, given the small spatial scale of single plants known, repeated check lines could be included to provide an evaluation in comparison to best material, which is not feasible in large plots. The HTP data may allow plant breeders to better quantify plant growth and environmental conditions providing selection and modeling opportunities to understand plant growth (De Leon et al., 2016).

Within wheat breeding HTP methodology applied in early generations could provide breeding programs with five or more rounds of selection before material is widely tested. The use of pipelined analysis should allow trait extraction to be automated with minimal user intervention and time commitment. At these early stages of the plant breeding program large investments in time and resources is challenging. This study has focused on wheat and wheat breeding applications, yet these methods should be applicable to a wide range of crops. For example, crops that are clonally propagated such as potato (*Solanum tuberosum* L.) could benefit through individual analysis (Slater et al., 2017). An intermediate wheatgrass (*Thinopyrum intermedium*) breeding program that uses genomic selection could also complement their selection strategy by combining HTP data increasing selection strategy in a perennial crop (Crain et al., 2021b). For crops with extremely long growth cycles such as trees, the precision phenotyping could cost effectively increase breeding gains (Alves et al., 2020).

5 Conculsions

We have provided proof of concept for field-based, single plant phenotyping by modifying existing HTP pipelines. As new advancements further enhance HTP systems, breeders can combine this new data with computational resources for efficient phenotyping of plants ranging from segregating F_2 generations to fixed lines. As processing pipelines are further refined, plant breeding programs should be able to utilize HTP methods that scale to the size of the breeding program compared to time consuming phenotypic measurements or genotyping that would be infeasible in terms of cost and time for evaluating segregating material. This will greatly increase the amount and precision of data that can be used to drive genetic gain. The methodology utilized in this work should be applicable to a range of different crops and plant breeding programs, and allow the development of crops that can meet the world's food, fiber, and fuel needs.

Acknowledgments

This publication is supported by the EArly-concept Grants for Exploratory Research (EAGER) Grant No. 2019-67013-29008 from the USDA National Institute of Food and Agriculture (NIFA). The genomics work was performed on the Beocat Research Cluster at Kansas State University, which is funded in part by NSF grants CNS-1006860, EPS-1006860, EPS-0919443, ACI-1440548, CHE-1726332, and NIH P20GM113109. Contribution no. 22-047-J from the Kansas Agricultural Experiment Station.

Author Contribution

JC and JP provided conceptualization and methodology. BE implemented, man-

aged, and phenotyped field trials. JC and XW conducted formal analysis. JC prepared the original draft with all authors reviewing, editing, and approving the final manuscript.

Conflict of Interest

The authors declare no conflict of interest. Any opinions, findings, conclusions, or recommendations expressed in this publication are those of the authors and do not necessarily reflect the view of the U.S. Department of Agriculture.

Supplemental Material

Supplementary Table 1. Broad-sense heritability of high-throughput phenotyping data collected throughout the growing season with an unmanned aerial vehicle in association mapping (AM) and single plant (SPAM) panels, Manhattan, KS.

Season	Date	Trial	
		AM	SPAM
2018-2019	3 January	0.23	
	12 April	0.60	
	19 April	0.49	
	22 April		0.42
	24 April	0.54	0.50
	2 May	0.77	0.53
	10 May	0.40	0.50
	16 May	0.52	
	20 May	0.87	
	22 May	0.84	0.49
	30 May	0.72	0.43
	5 June	0.69	
	12 June	0.40	
	17 June	0.80	
	24 June	0.83	
2019-2020	20 March	0.27	
	1 April	0.23	
	9 April		0.32
	11 April	0.19	0.29
	23 April	0.54	0.25
	3 May	0.36	0.19
	8 May	0.54	0.17
	18 May	0.54	
	19 May		0.12
	23 May	0.58	0.08
	5 June	0.77	0.32
	11 June	0.75	0.36
	12 June	0.79	

Supplementary Table 2. Correlation between normalized difference vegetation index collected with high throughput phenotyping and wheat grain yield for full plots (AM) and single plants (SPAM) for two growing seasons of observations (2018-19, 2019-20). The SPAM trial includes both correlation to single plants and the correlation to full plot yields.

		AM trial	SPAM trial	
Season	**Date**	**AM Yield**	**SPAM Yield**	**AM Yield**
2018-2019	3 January	-0.02		
	12 April	-0.1		
	19 April	0.1		
	22 April		0.61***	-0.38***
	24 April	0.28***	0.65***	-0.40***
	2 May	0.35***	0.69***	-0.38***
	10 May	0.15**	0.74***	-0.39***
	16 May	0.41***		
	20 May	0.52***		
	22 May	0.52***	0.72***	-0.38***
	30 May	0.60***	0.59***	-0.31***
	5 June	0.55***		
	12 June	0.51***		
	17 June	0.46***		
	24 June	0.06		
2019-2020	20 March	-0.22***		
	1 April	-0.20***		
	9 April		0.32***	0.01
	11 April	-0.02	0.35***	0.02
	23 April	0.24***	0.17**	0.04
	3 May	0.09	0.44***	0.05
	8 May	0.27***	0.48***	0.02
	18 May	0.23***		
	19 May		0.48***	0.06
	23 May	0.30***	0.52***	0.03
	5 June	0.63***	0.50***	0.04
	11 June	0.56***	0.47***	0.05
	12 June	0.55***		

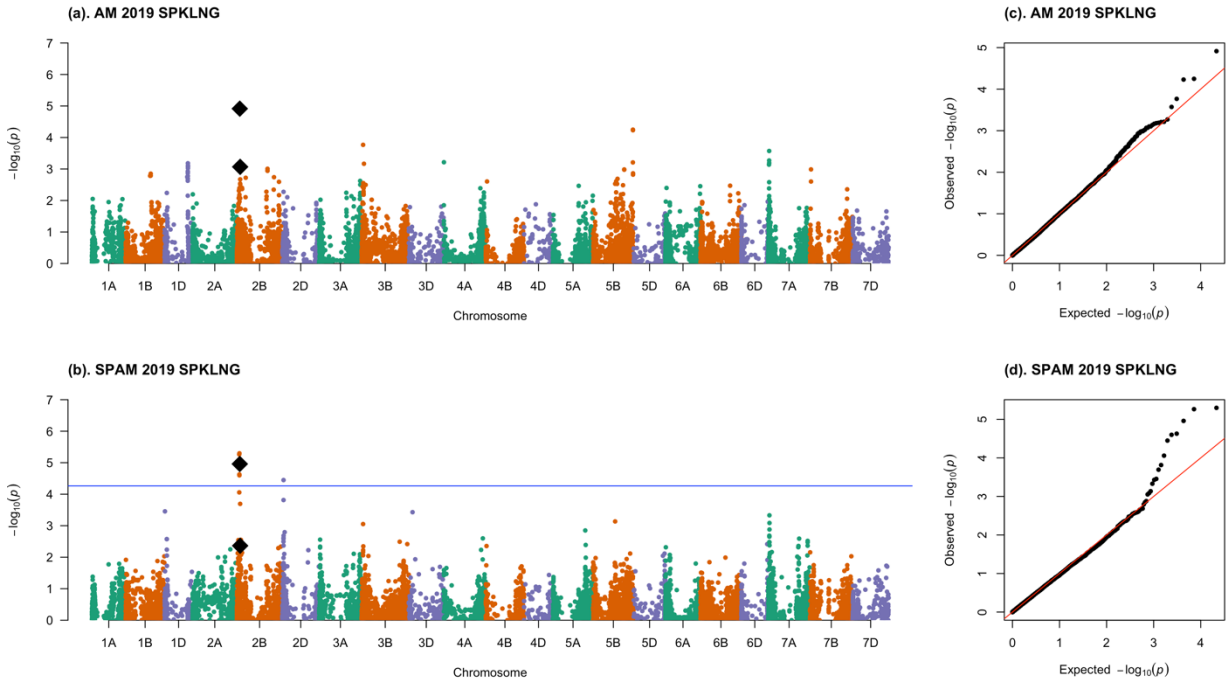

Supplementary Figure 1. Manhattan plots of spike length with phenotypic data taken from full plots (a) and single plots (b). Markers above significance threshold, false discovery rate (FDR = 0.1), in each panel have been highlighted with larger marker character. Quantile-quantile plots showing the expected and observed residual distribution for each genome-wide association analysis (c and d).

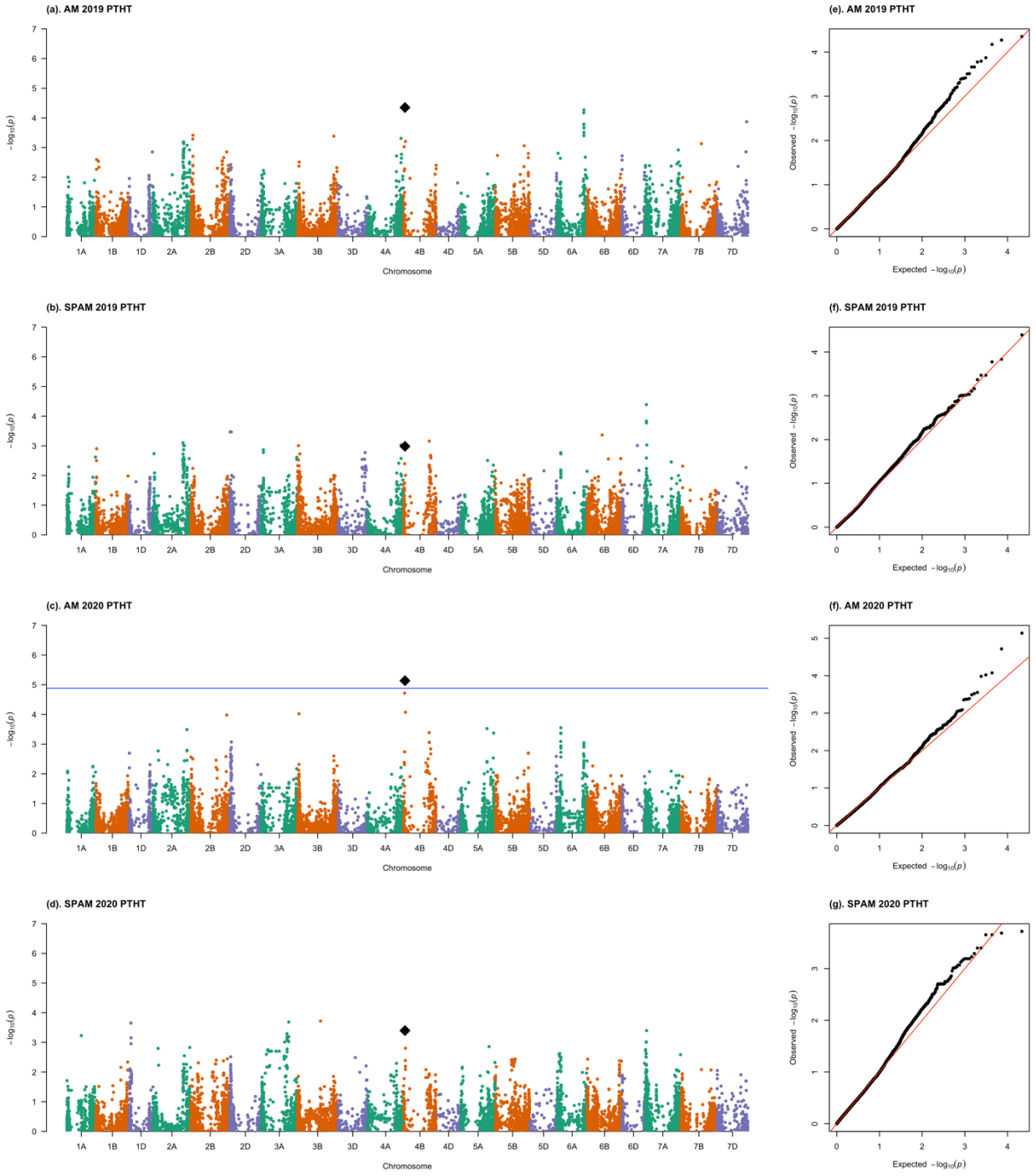
(a). AM 2019 PTHT
(b). SPAM 2019 PTHT
(c). AM 2020 PTHT
(d). SPAM 2020 PTHT
(e). AM 2019 PTHT
(f). SPAM 2019 PTHT
(f). AM 2020 PTHT
(g). SPAM 2020 PTHT
Chromosome
1A 1B 1D 2A 2B 2D 3A 3B 3D 4A 4B 4D 5A 5B 5D 6A 6B 6D 7A 7B 7D
Observed $-\log_{10}(p)$
Expected $-\log_{10}(p)$

Supplementary Figure 2. Manhattan plots of plant height with phenotypic data taken from full plots (a, c) and single plots (b, d) in the 2018-19 and 2019-20 season. The highest scoring marker for all trials has been highlighted on chromosome 4B, with the genome-wide false discovery rate (FDR = 0.1) as a horizontal blue line. Quantile-quantile plots showing the expected and observed residual distribution for each genome-wide association analysis (e and f)

References

Alves, F.C., K.M. Balmant, M.F.R. Resende, M. Kirst, and G. de los Campos. 2020. Accelerating forest tree breeding by integrating genomic selection and greenhouse phenotyping. Plant Genome 13(3): 1–13. doi: 10.1002/tpg2.20048.Andrade-Sanchez, P., M.A. Gore, J.T. Heun, K.R. Thorp, A.E. Carmo-Silva, et al. 2014. Development and evaluation of a field-based high-throughput phenotyping platform. Funct. Plant Biol. 41(1): 68–79. doi: 10.1071/FP13126.Babar, M.A., M. Van Ginkel, A.R. Klatt, B. Prasad, and M.P. Reynolds. 2006. The potential of using spectral reflectance indices to estimate yield in wheat grown under reduced irrigation. Euphytica 150(1–2): 155–172. doi: 10.1007/s10681-006-9104-9.Barker, J., N. Zhang, J. Sharon, R. Steeves, X. Wang, et al. 2016. Development of a field-based high-throughput mobile phenotyping platform. Comput. Electron. Agric. 122: 74–85. doi: 10.1016/j.compag.2016.01.017.Bates, D., M. Mächler, B. Bolker, and S. Walker. 2015. Fitting linear mixed-effects models using lme4. J. Stat. Softw. 67(1). doi: 10.18637/jss.v067.i01.Belamkar, V., M.J. Guttieri, W. Hussain, D. Jarquín, I. El-basyoni, et al. 2018. Genomic selection in preliminary yield trials in a winter wheat breeding program. G3 Genes, Genomes, Genet. 8(8): 2735–2747. doi: 10.1534/g3.118.200415.Bräutigam, A., and U. Gowik. 2010. What can next generation sequencing do for you? Next generation sequencing as a valuable tool in plant research. Plant Biol. 12(6): 831–841. doi: 10.1111/j.1438-8677.2010.00373.x.Browning, B.L., and S.R. Browning. 2016. Genotype imputation with millions of reference samples. Am. J. Hum. Genet. 98(1): 116–126. doi: 10.1016/j.ajhg.2015.11.020.Busemeyer, L., A. Ruckelshausen, K. Möller, A.E. Melchinger, K. V Alheit, et al. 2013. Precision phenotyping of biomass accumulation in triticale reveals temporal genetic patterns of regulation. Sci. Rep. 3: 2442. doi: 10.1038/srep02442.Chai, S., Q. Yao, X. Zhang, X. Xiao, X. Fan, et al. 2021. The semi-dwarfing gene Rht-dp from dwarf polish wheat (Triticum polonicum L.) is the "Green Revolution" gene Rht-B1b. BMC Genomics 22(1): 1–15. doi: 10.1186/s12864-021-07367-x.Cobb, J.N., G. DeClerck, A. Greenberg, R. Clark, and S. McCouch. 2013. Next-generation phenotyping: requirements and strategies for enhancing our understanding of genotype-phenotype relationships and its relevance to crop improvement. Theor. Appl. Genet. 126(4): 867–887. doi: 10.1007/s00122-013-2066-0.Condon, A.G., M.P. Reynolds, J. Brennan, M. Van Ginkel, R. Trethowan, et al. 2008. Stomatal aperture related traits and yield potential in bread wheat. International Symposium on Wheat Yield Potential. p. 126Crain, J., P. Bajgain, J. Anderson, X. Zhang, L. DeHaan, et al. 2020. Enhancing crop domestication through genomic selection, a case study of intermediate wheatgrass.

Front. Plant Sci. 11(March): 1–15. doi: 10.3389/fpls.2020.00319.Crain, J., L. DeHaan, and J. Poland. 2021a. Genomic prediction enables rapid selection of high-performing genets in an intermediate wheatgrass breeding program. Plant Genome 14(2). doi: 10.1002/tpg2.20080.Crain, J., A. Haghighattalab, L. DeHaan, and J. Poland. 2021b. Development of whole-genome prediction models to increase the rate of genetic gain in intermediate wheatgrass (Thinopyrum intermedium) breeding. Plant Genome 14(2). doi: 10.1002/tpg2.20089.Crain, J., S. Mondal, J. Rutkoski, R.P. Singh, and J. Poland. 2018. Combining high-throughput phenotyping and genomic information to increase prediction and selection accuracy in wheat breeding. Plant Genome 11(1): 1–14. doi: 10.3835/plantgenome2017.05.0043.Crain, J., M. Reynolds, and J. Poland. 2017. Utilizing high-throughput phenotypic data for improved phenotypic selection of stress-adaptive traits in wheat. Crop Sci. 57(2): 648–659. doi: 10.2135/cropsci2016.02.0135.Crain, J.L., Y. Wei, J. Barker, S.M. Thompson, P.D. Alderman, et al. 2016. Development and deployment of a portable field phenotyping platform. Crop Sci. 56(3): 965–975. doi: 10.2135/cropsci2015.05.0290.Crossa, J., R. Fritsche-Neto, O.A. Montesinos-Lopez, G. Costa-Neto, S. Dreisigacker, et al. 2021. The modern plant breeding triangle: optimizing the use of genomics, phenomics, and enviromics data. Front. Plant Sci. 12(April): 1–6. doi: 10.3389/fpls.2021.651480.Deery, D., J. Jimenez-Berni, H. Jones, X. Sirault, and R. Furbank. 2014. Proximal remote sensing buggies and potential applications for field-based phenotyping. Agronomy 4(3): 349–379. doi: 10.3390/agronomy4030349.Deery, D.M., and H.G. Jones. 2021. Field phenomics: will it enable crop improvement? Plant Phenomics 2021. doi: 10.34133/2021/9871989.Donald, C.M. 1968. The breeding of crop ideotypes. Euphytica 17(3): 385–403. doi: 10.1007/BF00056241.Duddu, H.S.N., E.N. Johnson, C.J. Willenborg, and S.J. Shirtliffe. 2019. High-throughput UAV image-based method is more precise than manual rating of herbicide tolerance. Plant Phenomics 2019: 1–9. doi: 10.34133/2019/6036453.Van Eeuwijk, F.A., D. V. Bustos-Korts, and M. Malosetti. 2016. What should students in plant breeding know about the statistical aspects of genotype × Environment interactions? Crop Sci. 56(5): 2119–2140. doi: 10.2135/cropsci2015.06.0375.Elias, A.A., K.R. Robbins, R.W. Doerge, and M.R. Tuinstra. 2016. Half a century of studying genotype × environment interactions in plant breeding experiments. Crop Sci. 56(5): 2090–2105. doi: 10.2135/cropsci2015.01.0061.Enciso-Rodriguez, F., D. Douches, M. Lopez-Cruz, J. Coombs, and G. de los Campos. 2018. Genomic selection for late blight and common scab resistance in tetraploid potato (Solanum tuberosum). G3 Genes, Genomes, Genet. 8(7): 2471–2481. doi: 10.1534/g3.118.200273.Endelman, J.B. 2011. Ridge regression and other kernels for genomic selection with R package rrBLUP. Plant Genome J. 4(3): 250–255. doi: 10.3835/plantgenome2011.08.0024.Endelman, J.B., and J.L. Jannink. 2012. Shrinkage estimation of the realized relationship matrix. GenesGenomes-Genetics 2(11): 1405–1413. doi: 10.1534/g3.112.004259.Fahlgren, N., M.A. Gehan, and I. Baxter. 2015. Lights, camera, action: High-throughput plant phenotyping is ready for a close-up. Curr. Opin. Plant Biol. 24: 93–99. doi: 10.1016/j.pbi.2015.02.006.Fischer, R.A., and G.J. Rebetzke. 2018. Indirect

selection for potential yield in early-generation, spaced plantings of wheat and other small-grain cereals: A review. Crop Pasture Sci. 69(5): 439–459. doi: 10.1071/CP17409.Furbank, R.T., and M. Tester. 2011. Phenomics - technologies to relieve the phenotyping bottleneck. Trends Plant Sci. 16(12): 635–644. doi: 10.1016/j.tplants.2011.09.005.Glaubitz, J.C.J., T.M.T. Casstevens, F. Lu, J. Harriman, R.R.J. Elshire, et al. 2014. TASSEL-GBS: A high capacity genotyping by sequencing analysis pipeline. PLoS One 9(2): e90346. doi: 10.1371/journal.pone.0090346.Grogan, S.M., J. Anderson, P. Stephen Baenziger, K. Frels, M.J. Guttieri, et al. 2016. Phenotypic plasticity of winter wheat heading date and grain yield across the US great plains. Crop Sci. 56(5): 2223–2236. doi: 10.2135/cropsci2015.06.0357.Guttieri, M.J., P. Stephen Baenziger, K. Frels, B. Carver, B. Arnall, et al. 2015. Variation for grain mineral concentration in a diversity panel of current and historical great plains hard winter wheat germplasm. Crop Sci. 55(3): 1035–1052. doi: 10.2135/cropsci2014.07.0506.Haghighattalab, A., L. González Pérez, S. Mondal, D. Singh, D. Schinstock, et al. 2016. Application of unmanned aerial systems for high throughput phenotyping of large wheat breeding nurseries. Plant Methods 12(1): 35. doi: 10.1186/s13007-016-0134-6.Heffner, E.L., A.J. Lorenz, J.L. Jannink, and M.E. Sorrells. 2010. Plant breeding with genomic selection: gain per unit time and cost. Crop Sci. 50(5): 1681–1690. doi: 10.2135/cropsci2009.11.0662.Heffner, E.L., M.E. Sorrells, and J.-L.L. Jannink. 2009. Genomic selection for crop improvement. Crop Sci. 49(1): 1. doi: 10.2135/cropsci2008.08.0512.Heslot, N., J.L. Jannink, and M.E. Sorrells. 2015. Perspectives for genomic selection applications and research in plants. Crop Sci. 55(1): 1–12. doi: 10.2135/cropsci2014.03.0249.Holland, J.B., W.E. Nyquist, and C.T. Cervantes-Martínez. 2010. Estimating and interpreting heritability for plant breeding: an update. Plant Breeding Reviews. p. 9–112International Wheat Genome Sequencing Consortium. 2014. A chromosome-based draft sequence of the hexaploid bread wheat (Triticum aestivum) genome. Science 345(6194): 1251788. doi: 10.1126/science.1251788.Jobson, E.M., R.E. Johnston, A.J. Oiestad, J.M. Martin, and M.J. Giroux. 2019. The impact of the wheat Rht-B1b semi-dwarfing allele on photosynthesis and seed development under field conditions. Front. Plant Sci. 10(February): 1–12. doi: 10.3389/fpls.2019.00051.Kang, M.S. 1997. Using genotype-by-environment interaction for crop cultivar development. Adv. Agron. 62(C): 199–252. doi: 10.1016/S0065-2113(08)60569-6.Krause, M.R., L. González-Pérez, J. Crossa, P. Pérez-Rodríguez, O. Montesinos-López, et al. 2019. Hyperspectral reflectance-derived relationship matrices for genomic prediction of grain yield in wheat. G3 Genes, Genomes, Genet. 9(4): 1231–1247. doi: 10.1534/g3.118.200856.Krause, M.R., S. Mondal, J. Crossa, R.P. Singh, F. Pinto, et al. 2020. Aerial high-throughput phenotyping enables indirect selection for grain yield at the early generation, seed-limited stages in breeding programs. Crop Sci. 60(6): 3096–3114. doi: 10.1002/csc2.20259.Lenth, R. V. 2020. emmeans: Estimated marginal means, aka least-squares means. https://cran.r-project.org/package=emmeans.De Leon, N., J.L. Jannink, J.W. Edwards, and S.M. Kaeppler. 2016. Introduction to a special issue

on genotype by environment interaction. Crop Sci. 56(5): 2081–2089. doi: 10.2135/cropsci2016.07.0002in.Liebisch, F., N. Kirchgessner, D. Schneider, A. Walter, and A. Hund. 2015. Remote, aerial phenotyping of maize traits with a mobile multi-sensor approach. Plant Methods 11(1): 9. doi: 10.1186/s13007-015-0048-8.Lin, Z., B.J. Hayes, and H.D. Daetwyler. 2014. Genomic selection in crops, trees and forages: A review. Crop Pasture Sci. 65(11): 1177–1191. doi: 10.1071/CP13363.Meuwissen, T.H.E., B.J. Hayes, and M.E. Goddard. 2001. Prediction of total genetic value using genome-wide dense marker maps. Genetics 157(4): 1819–1829. doi: 11290733.Muleta, K.T., G. Pressoir, and G.P. Morris. 2019. Optimizing genomic selection for a sorghum breeding program in Haiti: A simulation study. G3 Genes, Genomes, Genet. 9(2): 391–401. doi: 10.1534/g3.118.200932.Parmley, K., K. Nagasubramanian, S. Sarkar, B. Ganapathysubramanian, and A.K. Singh. 2019. Development of optimized phenomic predictors for efficient plant breeding decisions using phenomic-assisted selection in soybean. Plant Phenomics 2019: 1–15. doi: 10.34133/2019/5809404.Piepho, H.P., and J. Möhring. 2007. Computing heritability and selection response from unbalanced plant breeding trials. Genetics 177(3): 1881–1888. doi: 10.1534/genetics.107.074229.Pingali, P.L. 2012. Green Revolution: Impacts, limits, and the path ahead. Proc. Natl. Acad. Sci. U. S. A. 109(31): 12302–12308. doi: 10.1073/pnas.0912953109.Poland, J. 2015. Breeding-assisted genomics. Curr. Opin. Plant Biol. 24: 119–124. doi: 10.1016/j.pbi.2015.02.009.Poland, J.A., P.J. Brown, M.E. Sorrells, and J.L. Jannink. 2012a. Development of high-density genetic maps for barley and wheat using a novel two-enzyme genotyping-by-sequencing approach. PLoS One 7(2). doi: 10.1371/journal.pone.0032253.Poland, J., J. Endelman, J. Dawson, J. Rutkoski, S.Y. Wu, et al. 2012b. Genomic selection in wheat breeding using genotyping-by-sequencing. Plant Genome 5(3): 103–113. doi: Doi 10.3835/Plantgenome2012.06.0006.Prasad, B., B.F. Carver, M.L. Stone, M.A. Babar, W.R. Raun, et al. 2007. Potential use of spectral reflectance indices as a selection tool for grain yield in winter wheat under great plains conditions. Crop Sci. 47(4): 1426–1440. doi: 10.2135/cropsci2006.07.0492.Quail, K.J., R.A. Fischer, and J.T. Wood. 1989. Early generation selection in wheat. I. Yield potential. Aust. J. Agric. Res. 40(6): 1117–1133. https://doi.org/10.1071/AR9891117.R Core Team. 2020. R: a language and environment for statistical computing. https://www.r-project.org/.Rajaram, S., N.E. Borlaug, and M. Van Ginkel. 2002. CIMMYT international wheat breeding. Bread wheat Improv. Prod. FAO, Rome: 103–117.Rebetzke, G.J., A.G. Condon, R.A. Richards, and G.D. Farquhar. 2002. Selection for reduced carbon isotope discrimination increases aerial biomass and grain yield of rainfed bread wheat. Crop Sci. 42(3): 739–745. doi: 10.2135/cropsci2002.7390.Rife, T.W., and J.A. Poland. 2014. Field book: an open-source application for field data collection on android. Crop Sci. 54(4): 1624–1627.Rincent, R., J.P. Charpentier, P. Faivre-rampant, E. Paux, J. Le Gouis, et al. 2018. Phenomic selection is a low-cost and high-throughput method based on indirect predictions: Proof of concept on wheat and poplar. G3 Genes, Genomes, Genet. 8(12): 3961–3972. doi: 10.1534/g3.118.200760.Rouse, J.W., R.H. Haas, J.A. Schell, D.W. Deering,

and others. 1974. Monitoring vegetation systems in the Great Plains with ERTS. NASA Spec. Publ. 351(1974): 309–317.Rutkoski, J., J. Benson, Y. Jia, G. Brown-Guedira, J. Jannink, et al. 2012. Evaluation of genomic prediction methods for fusarium head blight resistance in wheat. Plant Genome J. 5(2): 51. doi: 10.3835/plantgenome2012.02.0001.Rutkoski, J., J. Poland, S. Mondal, E. Autrique, L. González Párez, et al. 2016. Canopy temperature and vegetation indices from high-throughput phenotyping improve accuracy of pedigree and genomic selection for grain yield in wheat. GenesGenomesGenetics 6(9): 2799–2808. doi: 10.1534/g3.116.032888.Rutkoski, J.E., J.A. Poland, R.P. Singh, J. Huerta-espino, S. Bhavani, et al. 2014. Genomic selection for quantitative adult plant stem rust resistance in wheat. Plant Genome J. 7(3): 1–10. doi: 10.3835/plantgenome2014.02.0006.Singh, D., X. Wang, U. Kumar, L. Gao, M. Noor, et al. 2019. High-throughput phenotyping enabled genetic dissection of crop lodging in wheat. Front. Plant Sci. 10(April): 1–11. doi: 10.3389/fpls.2019.00394.Slater, A.T., N.O.I. Cogan, B.C. Rodoni, H.D. Daetwyler, B.J. Hayes, et al. 2017. Breeding differently—the digital revolution: high-throughput phenotyping and genotyping. Potato Res. 60(3–4): 337–352. doi: 10.1007/s11540-018-9388-x.Stevenson, J.R., N. Villoria, D. Byerlee, T. Kelley, and M. Maredia. 2013. Green Revolution research saved an estimated 18 to 27 million hectares from being brought into agricultural production. Proc. Natl. Acad. Sci. U. S. A. 110(21): 8363–8368. doi: 10.1073/pnas.1208065110.Storey, J.D., and R. Tibshirani. 2003. Statistical significance for genomewide studies. 100(15): 6. doi: 10.1073/pnas.91.25.12091.Tanger, P., S. Klassen, J.P. Mojica, J.T. Lovell, B.T. Moyers, et al. 2017. Field-based high throughput phenotyping rapidly identifies genomic regions controlling yield components in rice. Sci. Rep. 7(June 2016): 1–8. doi: 10.1038/srep42839.Tattaris, M., M.P. Reynolds, and S.C. Chapman. 2016. A direct comparison of remote sensing aproaches for high-throughput phenotyping in plant breeding. Front. Plant Sci. 7(August): 1131. doi: 10.3389/fpls.2016.01131.The Royal Society. 2009. Reaping the benefits: science and the sustainable intensification of gloabl agriculutre. London.Turner, S. 2017. qqman: Q-Q and Manhattan Plots for GWAS Data. https://cran.r-project.org/package=qqman.Volpato, L., F. Pinto, L. González-Pérez, I.G. Thompson, A. Borém, et al. 2021. High throughput field phenotyping for plant height using UAV-based RGB imagery in wheat breeding lines: feasibility and validation. Front. Plant Sci. 12(February). doi: 10.3389/fpls.2021.591587.Wang, X., P. Silva, N.M. Bello, D. Singh, B. Evers, et al. 2020. Improved accuracy of high-throughput phenotyping from unmanned aerial systems by extracting traits directly from orthorectified images. Front. Plant Sci. 11(October): 1–14. doi: 10.3389/fpls.2020.587093.Wang, X., K.R. Thorp, J.W. White, A.N. French, and J.A. Poland. 2016. Approaches for geospatial processing of field-based high-throughput plant phenomics data from ground vehicle platforms. Trans. ASABE 59(5): 1053–1067. doi: 10.13031/trans.59.11502.Wang, X., H. Xuan, B. Evers, S. Shrestha, R. Pless, et al. 2019. High-throughput phenotyping with deep learning gives insight into the genetic architecture of flowering time in wheat. Gigascience 8(11). doi: 10.1093/gigascience/giz120.White, J.W., P. Andrade-sanchez, M.A. Gore, K.F.

Bronson, T.A. Coffelt, et al. 2012. Field-based phenomics for plant genetics research. F. Crop. Res. 133: 101–112. doi: 10.1016/j.fcr.2012.04.003.White, J.W., and M.M. Conley. 2013. A flexible, low-cost cart for proximal sensing. Crop Sci. 53(4): 1646–1649. doi: 10.2135/cropsci2013.01.0054.Wu, H., T. Wiesner-Hanks, E.L. Stewart, C. DeChant, N. Kaczmar, et al. 2019. Autonomous detection of plant disease symptoms directly from aerial imagery. Plant Phenome J. 2(1): 1–9. doi: 10.2135/tppj2019.03.0006.Yu, J., G. Pressoir, W.H. Briggs, I. Vroh Bi, M. Yamasaki, et al. 2006. A unified mixed-model method for association mapping that accounts for multiple levels of relatedness. Nat. Genet. 38(2): 203–8. doi: 10.1038/ng1702.Zadoks, J.C., T.T. Chang, and C.F. Konzak. 1974. A decimal code for the growth stages of cereals. Weed Res. 14(6): 415–421. doi: 10.1111/j.1365-3180.1974.tb01084.x.Zhang, Z., E. Ersoz, C.Q. Lai, R.J. Todhunter, H.K. Tiwari, et al. 2010. Mixed linear model approach adapted for genome-wide association studies. Nat. Genet. 42(4): 355–60. doi: 10.1038/ng.546.Zhang, X., P. Pérez-rodríguez, J. Burgueño, M. Olsen, E. Buckler, et al. 2017. Rapid cycling genomic selection in a multiparental tropical maize population. G3 Genes, Genomes, Genet. 7(7): 2315–2326. doi: 10.1534/g3.117.043141.Zhu, X., W.L. Leiser, V. Hahn, and T. Würschum. 2021. Phenomic selection is competitive with genomic selection for breeding of complex traits. Plant Phenome J. 4(1): 1–21. doi: 10.1002/ppj2.20027.

Figures and Tables